International Journal on Interactive Design and Manufacturing (IJIDeM) (2024) 18:4189–4208
https://doi.org/10.1007/s12008-024-01958-0

ORIGINAL ARTICLE

A new interactive design method for carbon fibres laminate component

Daniele Landi[1]

Received: 27 September 2023 / Accepted: 11 June 2024 / Published online: 29 June 2024

Abstract
Carbon fibre is the most common reinforcing phase in composite materials. However, it is difficult to determine the performance parameters of a monofilament. This paper provides an efficient method for performing the global layup optimization of composite laminates, considering the relationship between material characteristics and process parameters. In particular, a new method is proposed that, by integrating commercial tools, can support designers in the design and construction of carbon fibre components. The approach involves four functional groups that interact with each other: requirements and specifications, material definition, process implementation, and design and simulation. The idea is to create a continuous process to realize continuous product optimization. The approach was applied to the optimization of the front wing of a Formula 4 vehicle. After the validation method phase, through a comparison between real data and numerical simulations, product optimization was conducted. Different optimized solutions were obtained, and the solution minimizing the mass but 'allowing the vehicle to bear stress and strain values within the required limits was chosen. This methodology can be applied to support the designer during both the early design phase and the optimization phase of laminated products.

Keywords Carbon fibre · Laminate optimization · Combined finite discrete element method · Multi-objective optimization · Lamina (ply) · Laminates

1 Introduction

Novel materials go hand in hand with improving technologies. Owing to their remarkable weight-to-strength ratio, carbon fibre-reinforced polymer (CFRP) composites are increasingly being used in transport since they create lighter, more fuel-efficient vehicles and have renewable energy applications and design projects. CRFPs are strategic for the European industry's growth and development: currently, they are being used in Airbus planes, BMW's electric vehicles, and Vestas' wind turbines.

The demand for CFRPs in 2016 was around 63,500 tons, which rose to 120,000 tons by 2022 with an average annual growth rate of 11% [1].

CFRPs are multiphase solid materials consisting of two or more materials with different physical and chemical properties, and the use of this material in different sectors (such as aerospace engineering, automotive industry, and racing sector) has increased in recent years [2].

In particular, in the CFRP, a matrix and a carbon fibre are always present. The matrix, generally of a polymeric nature, has the function of keeping the fibres in a fixed position and transferring and distributing the tension derived from the loads between the various fibres as a barrier against the external environment. The external environment can often be hostile to fibres when it introduces, for instance, humidity or chemical agents and protects the surface of the fibres from mechanical degradation that may be caused by abrasion.

Carbon fibre materials can exhibit anti-flammability properties due to the use of flame-retardant epoxy resins and other additives. Research has shown that carbon fibre-reinforced composites based on epoxy resins containing certain additives can possess intrinsic anti-flammability. Additionally, flame-retardant carbon fibre products are manufactured using flame-retardant epoxy resins that resist the spread of fire,

✉ Daniele Landi
daniele.landi@unibg.it

[1] Department of Management, Information and Production Engineering, Università Di Bergamo, Via Pasubio 7/B, 24044 Dalmine, BG, Italy

making them ideal for applications in which fire resistance is important [3–5].

For creating carbon fibre products it is possible to have different types of matrices, thermoplastics, thermosets, metals, and ceramics. The most used matrices are the thermosetting ones or rather the molecules linked together by strong chemical bonds that are formed during the polymerization reaction that occurs in the curing phase. These bonds, once they have formed, unlike thermoplastic matrices, cannot be dissolved by applying heat.

The fibres, whether they are carbon, glass, aramid, or boron, are the main constituent of a composite material, not only because they represent the main fraction of its volume, but also because they bear most of the applied load. For this reason, the correct choice of fibre type, length, volume fraction, and orientation is of fundamental importance, as it influences density, tensile or compression strength, fatigue strength, and cost.

Considering these reasons, it is necessary to develop a method to understand the performance of the product in function of a different matrix or fibre. Given the importance of fibre, the principal aim of this paper is to evaluate the importance of fibre type and direction in a real case study.

In the scientific literature, the theory of composite laminates is well established, and the macroscopic properties of composite materials can be deduced according to the properties and arrangements of the fibre and matrix [4, 6, 7]. Theories of laminates * MERGEFORMAT [8] often rely on mathematical models that make simplifying assumptions. These models typically ignore the stress distribution within the thickness of the laminate and impose specific boundary conditions to simplify the calculations. However, these simplifications can lead to inaccuracies and potential issues in predicting the material's real-world behavior, particularly under complex loading conditions. Under actual complex surfaces, the finite elements of micromechanics and macroscopic mechanics. Tang and Postle [9] proposed an analysis based on numerical simulation and mathematical modelling after the weaving model was established. Huang and Ramakrishna * MERGEFORMAT [10] proposed a versatile and easy-to-use microcomposite model that can simulate the elastic, elastoplastic, and stress limits of two-dimensional braided composites under arbitrary loads.

Donadon et al. [11] presented an analytical model for the prediction of the elastic behaviour of plain weave fabric composites based on classical laminate theory, and the theoretical predictions were compared with the experimental results and predictions using alternative models available in the literature. Chun et al. [12] examined the effects of z-pin reinforcement on the elastic properties of composite materials, as well as the changes in the elastic properties based on the diameter of the z-pin. Kamiński and Pawlak [13] proposed computational techniques based on the finite element method (FEM) solution to the cell problem to discover the sensitivities and uncertainties in the homogenized tensor that resulted from the variations of the material parameters in the CFRP. Further, Kamarudin and Ismail [14] established a three-dimensional (3D) finite element model of unidirectional fibre reinforced composites using a periodic boundary condition method to predict the elastic mechanical behaviour of a unit cell of such composites. Yang et al. * MERGEFORMAT [15] numerically simulated the tensile behaviour of a 3D orthogonal woven composite based on the unit cell model. The influence of crack damage and stress on the fibre, resin, and fibre–resin interface were analysed. Sun et al. [16] developed a multiscale computational analysis based on representative volume element modelling and molecular dynamics simulations to investigate the microscopic failure mechanisms of unidirectional CFRP composites.

However, these methods require a lot of time and computational resources, which makes them unsuitable for preliminary product design. Some rapid analysis methods have been integrated into layup optimization processes to counteract the large number of iteration cycles that are always required.

Furthermore, these methods can provide accurate information at a microscopic level or on some areas of the product. However, they are unable to simulate a real object made of carbon fibre in a rapid, precise, and intuitive way. These methods and tools have been developed to support researchers in the laboratory during different experimental tests but are not tools to support product or process design.

Todoroki and Ishikawa [17] used a response surface to obtain the buckling load with reduced computational costs. Hajmohammad et al. [18] employed an artificial neural network in their optimization to replace FEA (Finite Element Analysis) when determining the buckling load of composite plates. An alternative to these methods is the exact finite strip approach used to obtain buckling and post-buckling behaviour for prismatic plate assemblies [5–7].

The panel design package VICONOPT proposed by Butler and Williams [19], based on the exact finite strip method, was used by Liu et al. to create an optimum design for composite laminates [20].

These methods can be highly useful in optimization processes. However, it is significantly difficult to validate these approaches through experimental tests. The biggest limitation of these methods is the reproducibility and robustness of the approaches.

Over the past few decades, genetic algorithms (GAs) have been the most popular optimization techniques for composite structures. Different authors have presented approaches to optimize the buckling load, the strength of plates, or the weight and deformation of laminates [21, 23, 24]. These algorithms require a large amount of information that must be

robust and experimentally validated. Therefore, it was difficult to apply these tools in the early stages of design, during which not all the factors were known. It is also difficult to analyze the interaction between different possible solutions.

To overcome the limitations presented, in the present work, a new design methodology is presented to optimize CFRP artefacts. Through the use of a parametric CAD model, FEM solver, and optimizing module, it is possible to identify the best lamination of the component by considering all aspects of the product design.

The innovation proposed by this study enables interaction between the different design phases using commercial and easy-to-use tools. The idea is to provide not only highly accurate solutions but also a new design solution to be developed by engineers. The approach does not replace designers but supports the designers themselves when they consider all aspects connected to the world of composite materials, in particular carbon fibre. Aspects related to the material, geometry, and production of the product will, therefore, be taken into consideration. After this introduction, the paper is structured with the following chapters. Section 2 introduces the modelling strategy, proposing a new innovative method for evaluating materials and lamination and drape parameters. Subsequently, Sect. 3 applies the proposed methodology to optimize the front wing of a Formula 4 vehicle. Section 4 presents the optimization of the model, while Sect. 5 reports brief conclusions.

2 Modelling strategy

This paper proposes an interactive design process approach to support designers during the all-product phase definition. As described in the introduction, the correct definition of the product and process parameters is a key factor that can enhance product performance (in terms of mechanical characteristics) and process efficiency in order to reduce cost, energy consumption, waste, and marketing time.

Figure 1 describes the interactive approach to supporting the process design using a virtual model. The scope of this approach is to reduce the costs and time related to physical prototypes. However, the employment of virtual models requires the formalization and parameterization of the product structure using objected-oriented (O–O) analysis.

The approach involves four functional groups that interact with each other: requirements and specifications, material definition, process implementation, and design and simulation. The idea is to create a continuous process to achieve continuous product optimization. For the creation of a new product, the first step involves the definition of external input parameters. They are called external because they are not modifiable but represent constraints related to the customer, marketing, or mechanical requirements.

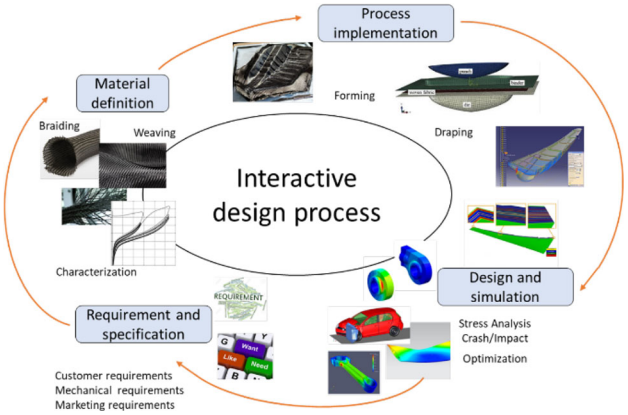

Fig. 1 The proposed interactive approach

Unlike materials defined as "conventional", such as metallic materials, which are generally used for structures and in which a mechanical behaviour is characterized by isotropy, the characteristics of composite materials depend on the orientation, number, type of fibre, and type of matrix used. Therefore, it is necessary to develop a tool capable of guiding designers in material choice, material direction, and fabric definition.

The module material definition is a database of composite materials with relative properties that support designers in choosing the correct material.

In the process implementation, the laminate is created. This phase is fundamental to the final characteristics of the finished product. Based on the initial specifications or requirements, as a function of the material and maximum permissible stress, deformation, and maximum displacement, the draping of the component is simulated. Depending on the number of layers, the thickness of the layers, and the orientation of the fibres, products with different mechanical characteristics can be obtained.

The orientation of the fibre is, in fact, the main parameter that characterizes the production of composite laminates, and it was only recently that the industry started to mandate additional parameters, such as porosity. Today, most commercial software products can define the orientation of the fibres in their mechanical simulations, at least for unidirectional materials, obtained from the drape analysis [25].

The design and simulation phases are involved in the simulation phase using a dedicated CAE tool, such as a FEM solver. The geometric model consists of a CAD assembly that includes all geometric details and data related to non-geometric parameters, such as materials, target temperature, and so on. Nongeometric information is added as an attribute to the property table of the CAD model. The import of product data into a CAD system can be seen as a common practice in virtual prototyping strategies. The development of CAD

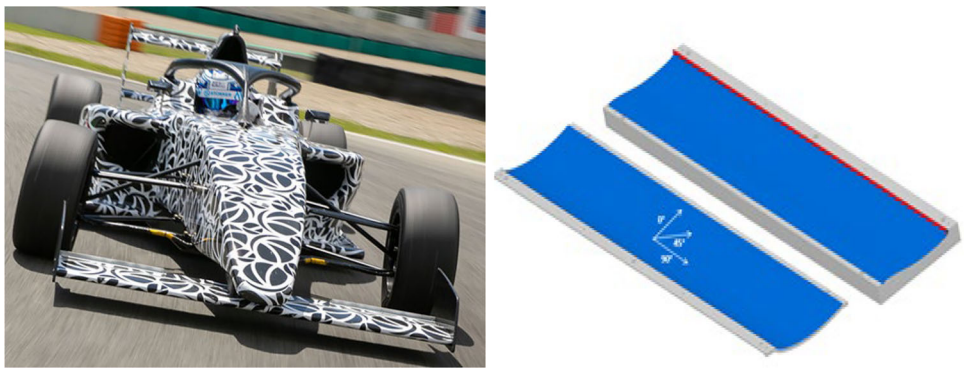

Fig. 2 Case study: front wing

models is a necessary step in the product development process. The proposed method considers geometric data with other physical and operative information to create an interaction between the design approach and the modelling and simulation phases.

In this phase (design simulation phase), the introduction of the concept of topology, as defined by Russo et al., may be useful [22]. Through numerical simulations, it is possible to find interactions between the way a structure is designed internally and its structural performance. Implementing the function–behaviour–structure (FBS) concept at this stage allows the designer to proceed to the next step of the approach.

To determine the optimal parameter configuration, a design optimization process was used. In this group, through optimization tools (DoE matrix and response surface methodology, among others), it is possible to identify the best configuration of parameters that guarantees a reliable process.

This approach aims to reduce the prototyping and testing of physical products. As highlighted in Fig. 1, the virtual prototyping and design optimization functional groups are connected with the real prototyping group. To obtain the correct result, it is necessary, in the first phase, to verify the validity of the virtual models. Further, at the end of the design flow, it is useful to verify the performance of the new process.

The interaction of such tools can fill the gap between traditional design methods and eco-innovation approaches to support the designer in decision-making activities.

3 Case study

To validate and present the main advantages of the proposed approach, the front wing of a Formula 4 car was analyzed. In the automotive sector and, in particular, the racing sector, the design process should consider the need to have high-speed production and high aerodynamic loads. The latter produces a high force on the wing. Other constraints related to the design are caused by regulations. Based on the race category, these constraints are shape limits, size limits, and maximum deformation limits, among others.

A wing is generally composed of three parts: the wing profile, bulkheads, and supports. The wing profile is composed of real surfaces that generate a downward thrust, while the bulkheads are parts placed at the two ends of the wing, which reduce the induced resistance and direct the air where it is most convenient for vehicle aerodynamics. Finally, the supports anchor the wing to the machine's body and must support the entire load generated to transfer it to the car.

The front wing used in this case study consists of two outer shells–one upper and one lower–made of carbon fibre composite material. Both are composed of three layers: (1) the first is carbon fibre, deposited above which is (2) a layer of filler (Fillcore) that does not perform a structural function but guarantees greater thickness and acts as a spacer for (3) the other layer of carbon fibre laminated above it. Figure 2 presents the mould and counter mould used to make shells; the part highlighted in red is the lip that will be used for gluing.

For the realization of both shells, after the lamination phase, the components are subjected to a vacuum cycle for 15 min for better cohesion between the layers. Then, they are autoclaved at a temperature of 120 °C and at 8.5 bar for a period of about 3 h.

The two shells enclose an insert, also in composite, with an internal composite omega shape. This part, which is generally of a commercial nature, is made using a single layer with a thickness of 0.8 mm in carbon fibre.

3.1 Material definition

Composite materials (composites for short) are made simultaneously by two or more materials with vastly different mechanical and/or chemical properties that remain separate and are clearly observable on a macroscopic or microscopic scale inside the finished part. Two categories of materials are involved: reinforce and filler. At least one piece from each category must be present. The filler surrounds and supports

Table 1 Comparison of mechanical properties of fibres

Type of fabric	Grammage (g/cm^2)
GG 200 T	200
GG 300 T	380
GG 800 T	800

reinforcement to maintain a mutual relative position. Reinforcement involves adding a special mechanical properties to improve the mechanical properties of the filler [26].

Fibre (carbon, glass, aramid, and borom, among others) is the main component of a composite material, not only because it is the main volume fraction, but also because it confers its technological and mechanical properties to the products. For this reason, the correct choice of fibre type, length, volume fraction, and orientation is highly important. It is possible to have short or long fibres.

To elaborate, short fibres have a lower cost and guarantee lower performance in terms of resistance and external finish because they do not guarantee good continuity in the component. They are generally used in lower-quality products and are arranged in a random direction, often using the spray-up technique–i.e., directly spraying the fibres together with the matrix on the open mould.

Long fibres are grouped into bundles that can then be arranged in this way or intertwined to obtain a fabric for the carbon fibres. With a long fibre, it is possible for the products to show high mechanical performance. However, resistance depends on fibre orientation.

Moreover, laminates are composite materials consisting of fillers and reinforcements in the form of fibres or fabrics. Fillers are used as resins of different types, depending on the application and desired properties. The most famous are polyester, vinyl ester, epoxy, phenol formaldehyde (PF), polyimide (PI), polyamide, polypropylene (PP), and polyether ether ketone (PEEK). They have different mechanical properties, different terms of use, thermal expansion, and resistance [27].

Considering the requirements and specifications for all racing cars of low weight, high resistance, and low deformation, a carbon fibre with a long fibre was chosen as the material. Different weaves with different properties have been selected, as shown in Table 1.

For each fabric, it is possible to define the mechanical properties, as indicated in Table 2, for GG300. Unlike common isotropic materials, for reinforced fabrics, it is necessary to define the properties along three main directions. Reported below are the mechanical properties of GG380 because the material of the real prototype is the object of this study. The other materials were altered to understand the variations in different parameters in the subsequent optimization phase.

Table 2 Mechanical properties of GG300T

Density			$1.7e^{-06}kg/mm^3$
Tsai–Wu coefficient			$-3.0e^{-06}mm^4/N^2$
Elastic constant	Young (E) module	E 1	59,800 MPa
		E 2	59,720 MPa
		E 3	/
	Poisson (ν) coefficient	ν 12	0.04
		ν 23	0.04
		ν 13	/
	Shear modulus (G)	G 12	3,300 MPa
		G 23	/
		G 13	/
Stress limit	Stress (ST)	ST 1	986.52 MPa
		ST 2	943.59 MPa
		ST 3	/
	Compression (SC)	SC 1	679.83 MPa
		SC 2	690.06 MPa
		SC 3	/
	Shear (SS)	SS 12	99.5 MPa
		SS 23	/
		SS 13	/

The mutual arrangement of the warp and weave creates three basic types of bonds, as presented in Fig. 3. The plain weave is the most rigid and pliable when the source in the warp and weave is equally strong and distant. The strand of weaving always passes over and under each strand of the warp (in other words, the balanced plain weave). Further, the twill weave is created by weaving crosses with at least two sources of the warp and reverting to one or more sources of the warp; in another place, the weaving moves right or left to the nearest spring warp. The fabric of a twill weave is more flexible but only in a soft surface arrangement of fibres. Finally, the satin weave is an integral textile link. The source of the warp is covered by four or more strands, the weave top, and one strand from the bottom. The surface of the fabric is smooth and shiny, with long pads in which the fibres lie parallel to the surface [28].

Fillcore, Ergal (aluminium), and PVC are isotropic materials. In the case of Fillcore, data related to stress limits used in the crisis criteria are not entered because it does not perform structural functions but is only a filler and will consequently be unstressed (Tables 3, 4, 5).

3.2 Process implementation

Starting with the specifications and defining the materials, the virtual geometric model for the next simulation and test was designed.

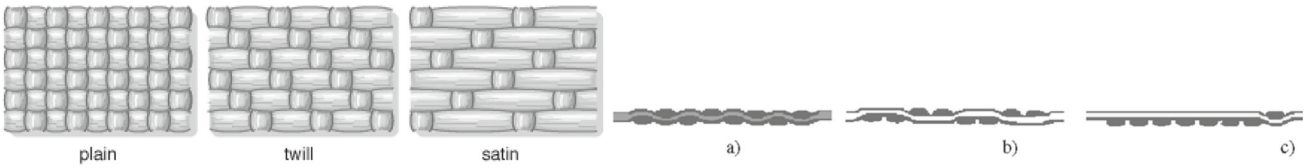

Fig. 3 Basic types of bonds

Table 3 Mechanical properties of Fillcore

Density		/
Elastic constant	Young (E) module	105 MPa
	Poisson (ν) coefficient	0.3
	Shear modulus (G)	/

Table 4 Mechanical properties of PVC component

Density		$1.4e^{-06}kg/mm^3$
Elastic constant	Young (E) module	3000 MPa
	Poisson (ν) coefficient	0.4
	Shear modulus (G)	/

Table 5 Mechanical properties of aluminium component

Density		$2.794e^{-06}kg/mm^3$
Elastic constant	Young (E) module	73,119 MPa
	Poisson (ν) coefficient	0.33
	Shear modulus (G)	/

The most critical part concerns the modelling of composite material geometries. Once the material is defined in the previous step, it is necessary to define the direction of the fibres, the number of layers, and the number of reinforcement zones.

This phase involves draping. The drapery simulation consists of the virtual "stretching" of various reinforcement layers defined by the layup through a calculation process, analyzing the defined rolling sequences, to obtain the orientation and distribution of the fibres along the surface of the model [29].

The drape analysis is performed using an appropriate calculation tool, usually implemented in FEM software packages for the design of composite laminates. The principal models adopted for fabric draping are geometrically composed and are called kinematic methods. These methods were first introduced in the 1950s by Mack and Taylor [30]. They adopt a simple kinematic algorithm through which the fabric is idealized as a net value obtained by superimposing two unidirectional layers, which represent the warp direction and the weft direction, and adapted to the geometric shape of the forming mould.

In addition, geometric approaches for draping are the most popular [29] due to the relative simplicity of the calculation method, which requires only a minimal input of data (such as the starting point of draping, geometry of the surface to be draped, and fibre directions).

However, despite the limitations present today in the models adopted for draping, they are able to make a substantial contribution to the design phase. This is because they allow the designer to virtually study the deposition of the various layers of fabric (or prepreg) on the moulds, enabling the analysis of the deformation (albeit in a limited manner) resulting from the forming process. This provides reliable information on the changes in the architecture of the fabric and, therefore, optimizes the structural properties of the composite products. It allows for maximizing both strength and material usage and, therefore, layup efficiency. It also allows the designer to analyze alternative draping processes, evaluate the use of different types of fabric, and characterize their limitations [31].

A strength of CFRP laminates is their possibility of optimizing the mechanical behaviour of the composite with respect to the specifications required for the material by suitably choosing the lamination sequence. However, the definition of the lamination sequence is characterized not only by the choice of fabric and/or its unidirectional orientation but also by the positioning of the reinforcement.

This procedure requires the management of the lamination "by zones"–i.e., modelling the lamination sequence by defining local lamination sequences, considering the various overlapping areas of the laminations. However, this approach–in addition to generating inefficiency, as it requires the designer to reinterpret the geometry and layup–can cause errors in the definition of the lamination, for which an approach defined as "for leathers" is increasingly preferred. This approach is substantially based on the methodology adopted in the technological process of lamination–i.e., of the successive stratification of shaped laminates to obtain the thickness of the laminate [32–34].

The front wing object of this study consists of two outer shells (one upper and one lower) composed of composite material. Both shells consist of three layers: the first is in contact with the mould on which the lamination is made using carbon fibre; above this, a layer of filler (Fillcore) is

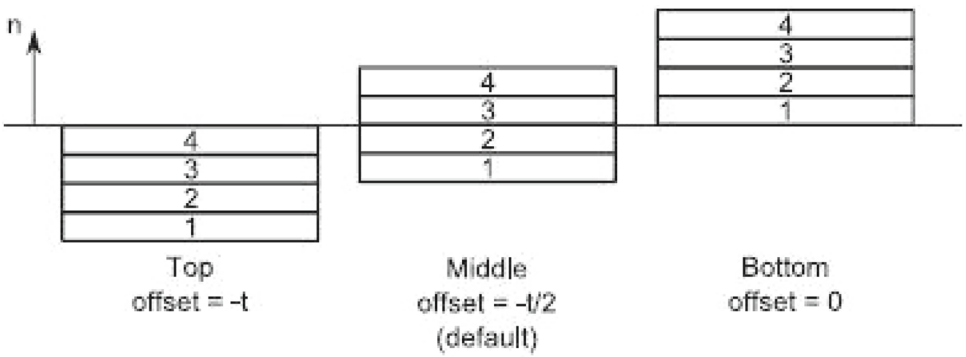

Fig. 4 Direction of virtual lamination: Top, middle, and bottom

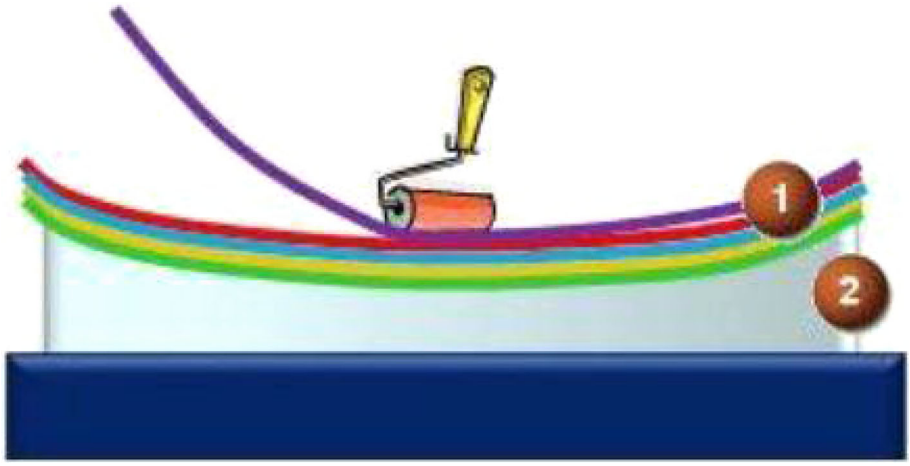

Fig. 5 External shape of the wing lamination process

deposited, which does not perform structural functions but guarantees greater thickness and acts as a spacer for the other layer of carbon fibre laminated above it. Figure 4 and Fig. 5 show the different virtual laminations. In function of the reference surface, it is possible to have a different lamination with different results of draping.

Figure 6 shows the lamination process of the case study. The top lamination was chosen starting from the reference surface. There are three different layers: two composite materials (i.e., GG380T) of 0.4 mm thickness and a central Fillcore of 0.5 mm thickness.

The angle orientation of the carbon fibre was chosen to be 0° for all the components. This was possible because the material used was a fabric with a fibre orientation of 0–90°. Then, the orientation angle did not modify the resistance of the component.

The internal support, omega, is a commercial component made with a single layer of GG380T E3-150N/40% 12K GX (TR50S) with a thickness of 0.8 mm.

3.3 Design and simulation

A coupled FEM analysis was performed to predict the general strength of the structure. The general-purpose NASTRAM 8.0 code was used as a computational tool to simulate the four-point bending test of the composite structure in the present study. The use of general FEM codes may yield a deeper analysis and enable structure development.

3.4 CAD Model

Figure 7 and Fig. 8 show the CAD model of the front wing considered in the present paper. The principal components are two external shells of composite material, two lateral side covers in aluminium, two PVC strips, four support inserts in Ergal, and one omega profile in carbon composite material.

The two shells are fixed by a system of bolts on one side, and a lip is made on the upper shell, which must only guarantee perfect coupling between the shells. Four holes are made at the centre of the upper shell, which allows the assembly with a group of reinforcing elements, such as the omega and four support inserts, among which are two PVC strips.

The omega is placed along the *y*-axis in contact with the lower and upper shells, guarantees better resistance to bending after a possible bending moment along *x axis*, and supports the upper shell, providing rigidity to the product.

In correspondence with the four holes made on it, the four Ergal inserts are positioned and perforated, and using bolts, they form a single body by fixing the omega to the upper shell.

Fig. 6 Lamination process

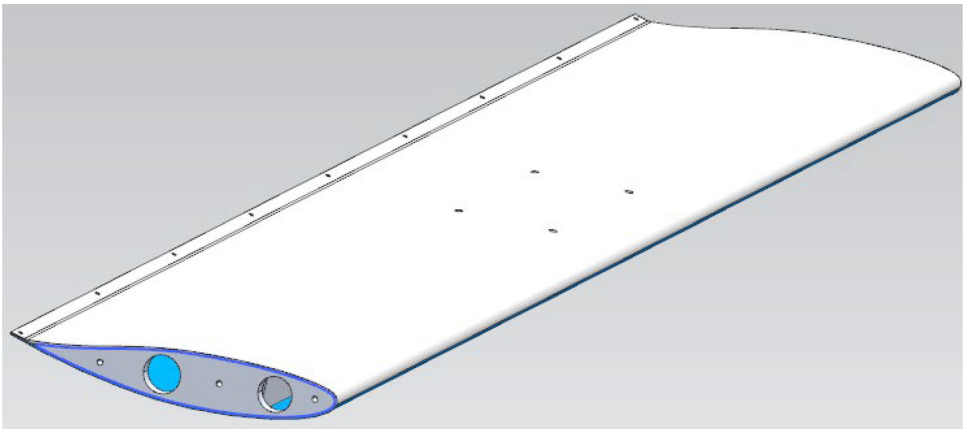

Fig. 7 CAD model of the analyzed product

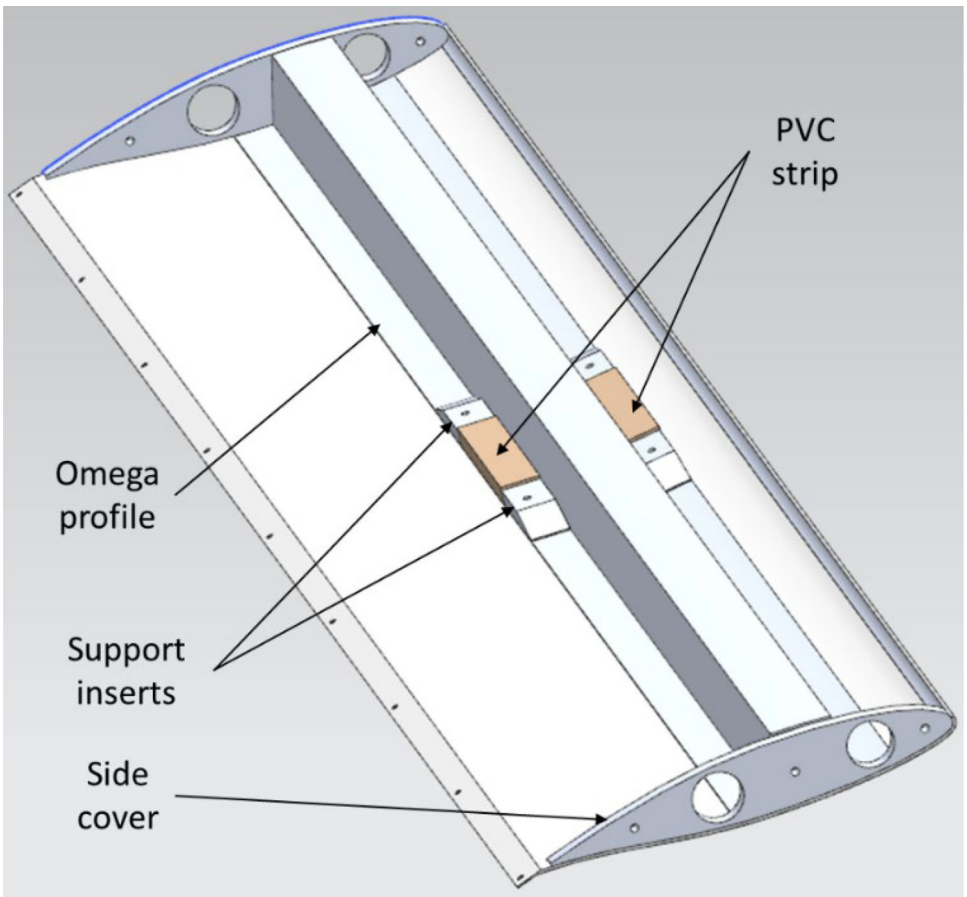

Fig. 8 Internal component of the front wing

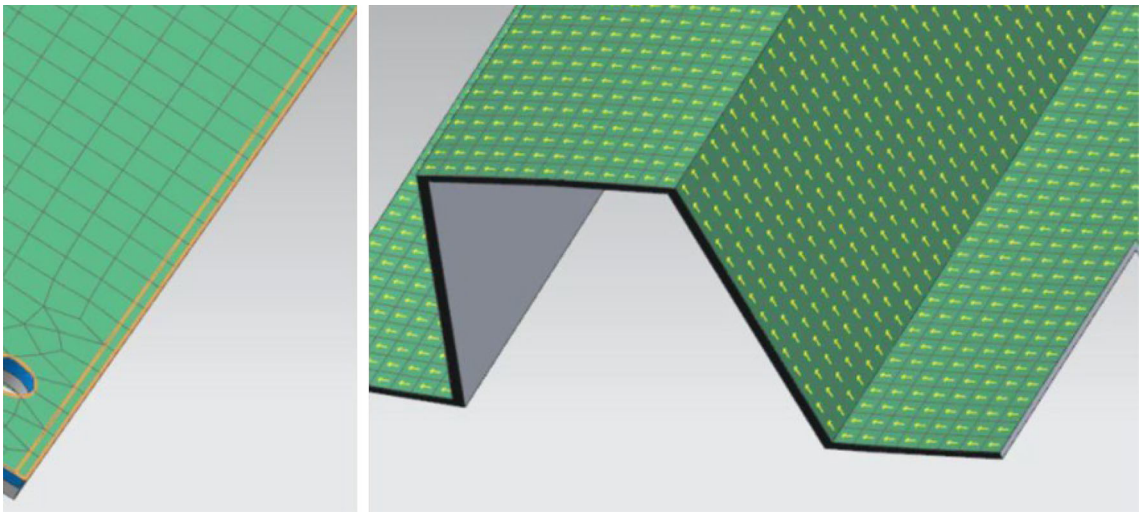

Fig. 9 Omega 2D mesh

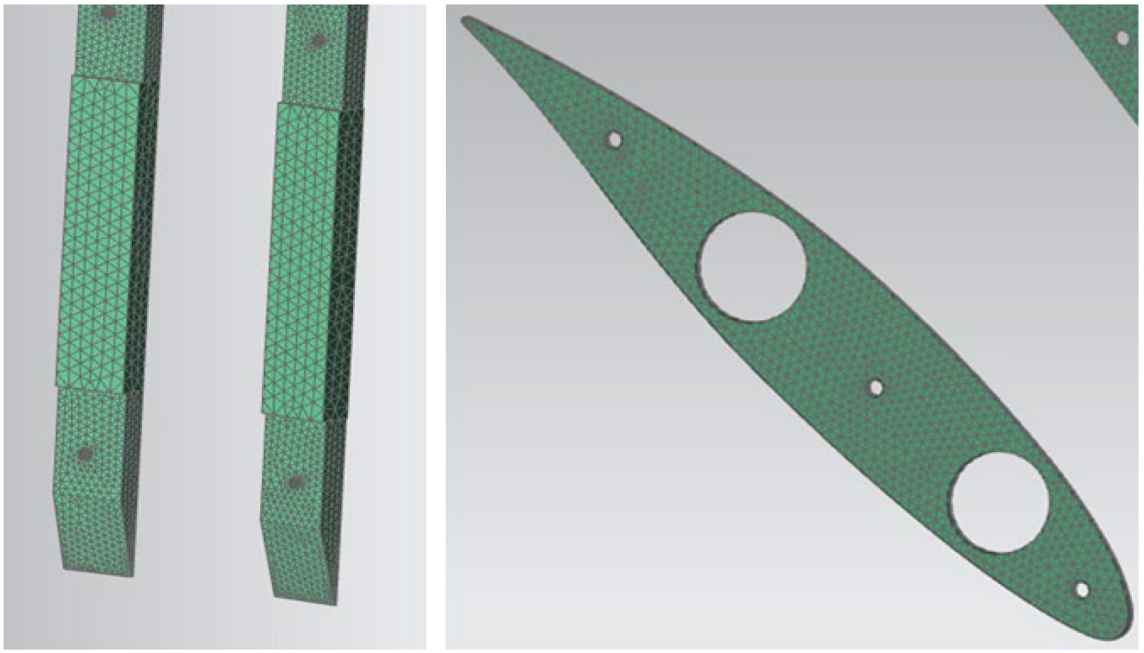

Fig. 10 Side cover (right figure), and support PVC insert (left figure),-strip 3D mesh

The strips are arranged between two pairs of inserts, such as vibration dampers or shock absorbers, since PVC is a thermoplastic material that does not have a structural function. They also prevent the inserts from moving excessively following the wing's deflection.

Finally, as a side cover for the two shells, two Ergal covers are always used, which are composed of profiles that are homologous to those of the lip and the two shells. The profiles also avoid possible corrugation of the shells while deforming during the work of the product.

The mesh of the carbon composite structure was generated using a triangular and rectangular element at four nodes with a maximum dimension of 3 mm (CQUAD4 element [35]) of the NASTRAM Library. The mesh, which had 5,368 rectangular and triangular elements with 15,551 nodes, was used to model the structure. Triangular elements were used to create interlaced joints at which fibre deposition occurred in several different directions. The details of the model of a single joint are given in Fig. 9 and Fig. 10. A single joint was divided into four different zones to calculate the correct material mechanical properties of the joint using the micromechanical theory of composites.

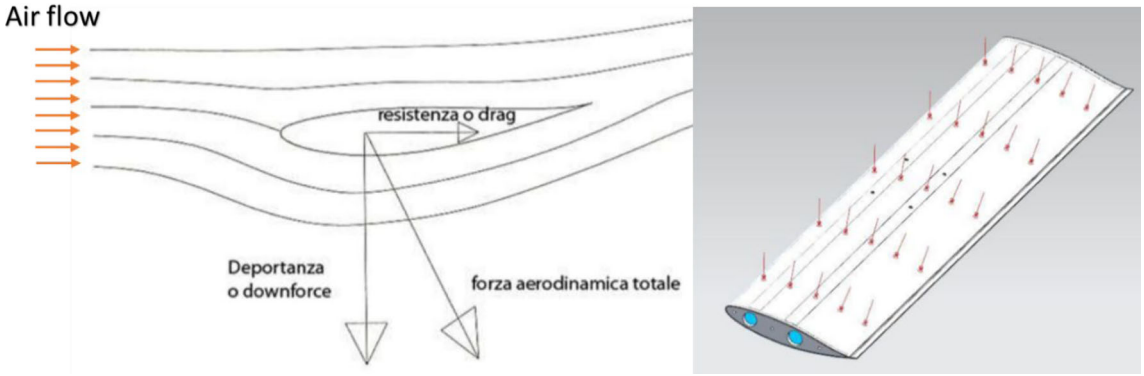

Fig. 11 Load applied to the wing

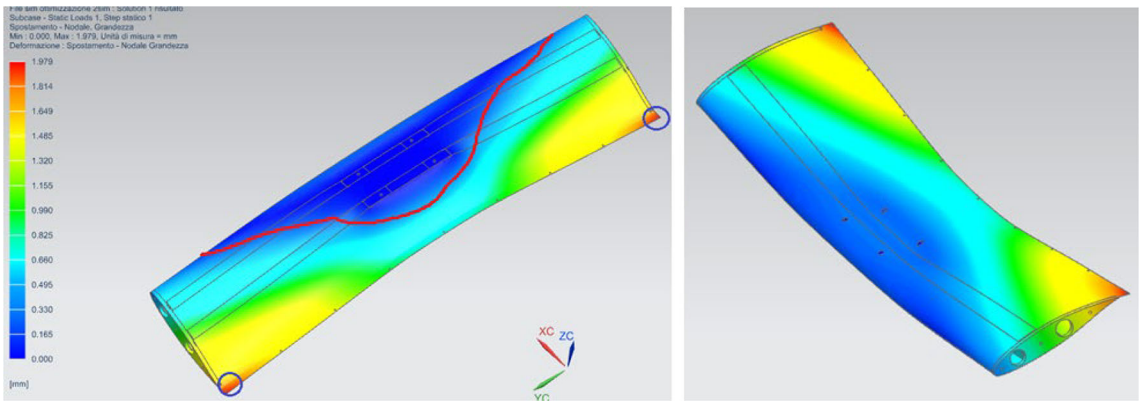

Fig. 12 Trend of deformation in the bottom (left) and upper surfaces of the wing

For the inserts, strips, and side covers, a 3D mesh was generated. A four-node tetrahedral element (CTETRA4 [35]) was chosen.

3.5 Boundary conditions

As required by the formula 4 race regulation, the front wing was fixed and loaded to simulate real behaviour. The constraint concerns fixing the internal support of the wing in correspondence with the four holes shown in Fig. 8. A pressure of 1000 Pa was applied as load to the upper surface of the wing directed downward, as indicated in Fig. 11. Pressure simulates the aerodynamic load during the use of a car. The magnitude of the load simulates the real case of interest.

3.6 Model validation

The result analysis concerns monitoring the stress, deformation, and failure coefficient. For the isotropic material, the von Mises criterion [36] was used, whereas for the laminate part, the Tsai–Wu criterion was used [37]. As described in the modelling strategy chapter, the aim of this paper is to create an interactive design process for a composite material object. However, it is necessary to validate a virtual model with experimental data to identify the correct simulation settings for the subsequent steps. The model was validated with the boundary condition described above and GG380T as the carbon material for the external shell. The real load was applied in the wind tunnel to reproduce real operating conditions.

Figure 12 illustrates the virtual deformation obtained throughout the virtual simulation. The deformation due to the applied load shows an increasing trend from the constraints.

Figure 13 shows the points where the real deformations were measured. Three lines were identified – orange, grey, and blue.i

Figure 14 shows the deformation trend along the z-axis obtained during the experimental tests. Given the symmetry of the product, only half points were reported. The zero position corresponds to the centre of the wing, where the holes used for wing fixing to the frame are located.

In the comparison between Figs. 14 and 15, a good correspondence between the real and virtual results is observed. From this first evaluation, it is possible to conclude that the virtual model is able to correctly simulate the real behaviour of the product.

In addition to the deformation analysis, through virtual simulations, the stress trend in the different components can be determined. Figure 16 shows the maximum stress on the

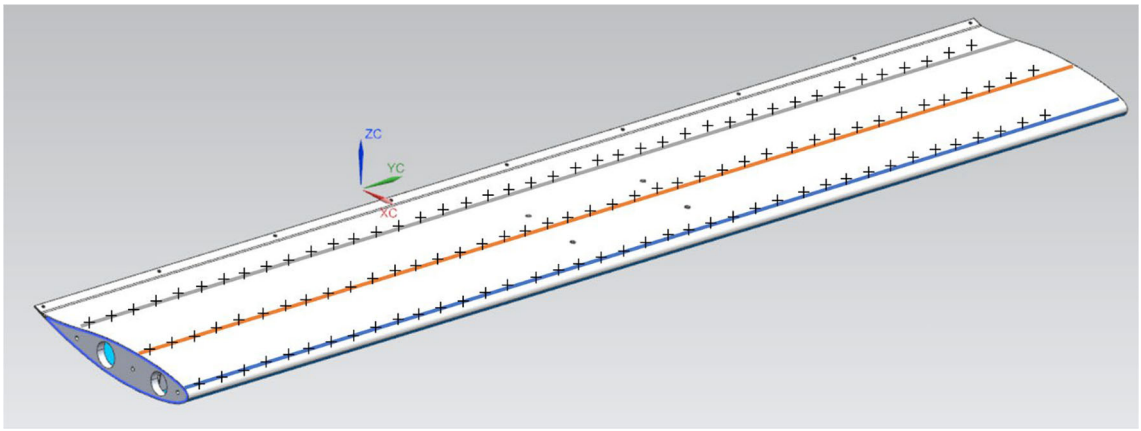

Fig. 13 Real measurement points

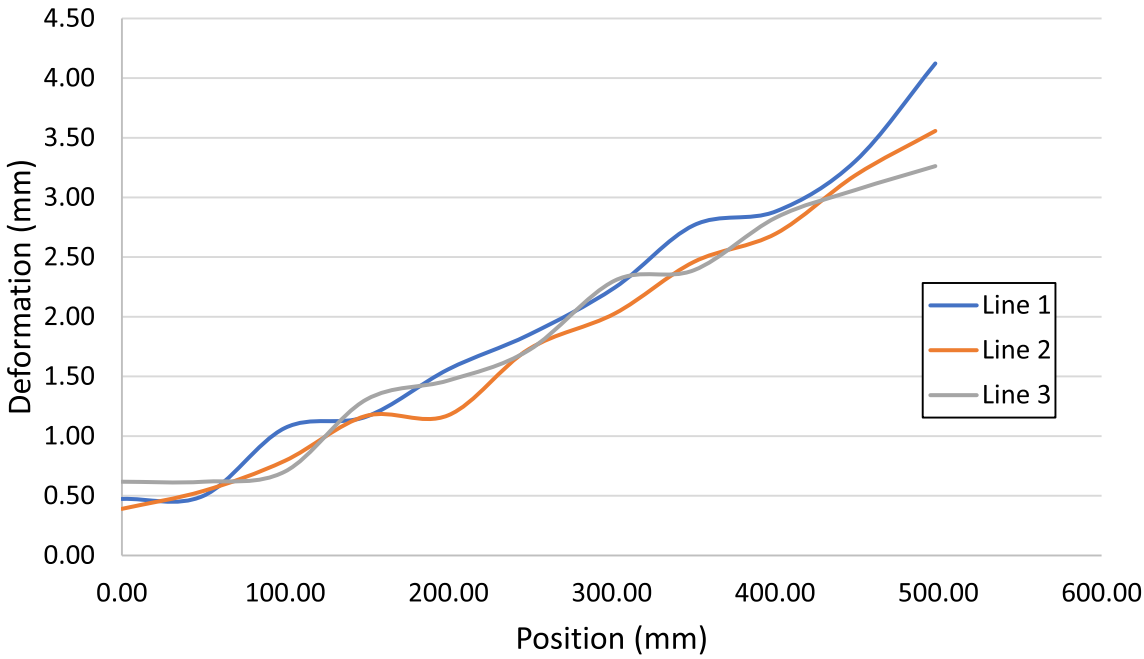

Fig. 14 Real deformation trend along the z-axis

two carbon layers of the wing shell. It is also possible to note a different value of stress on the external and internal layers.

The central layer in Fig. 17 is discharged. In fact, here, the Fillcore performs the function of the filler and has no structural functions, given its low mechanical properties.

On the side covers, almost no average stress is recorded, varying between 0 and 0.4 MPa. Generally, the part in contact with the upper shell is in traction, while the part below it is in compression, as shown in Fig. 18.

The same unloaded state is found in the PVC inserts because they do not have the function of supporting the load; they only act as spacers for the inserts where anchoring takes place. On the insert towards the lip area, a slight tendency for compression can be noticed, while on the opposite side, there are more tensile stresses even if stresses are close to zero.

Furthermore, the behaviour of the Ergal inserts is different. There are compression tensions of up to 4.3 MPa in the part in contact with the omega and points subjected to compression (7.5 MPa) in the upper part of the inserts towards the outside of the wing (as indicated by the red circles in Figs. 4 and 5). The Ergal insert, are the attachment sites of the structure, they are affected by more significant stresses owing to a load that is not particularly high.

Since these aforementioned elements are made with isotropic materials, the equivalent stress calculated according to the von Mises criterion can be considered. That the only stressed elements are the two Ergal inserts can be noticed (as

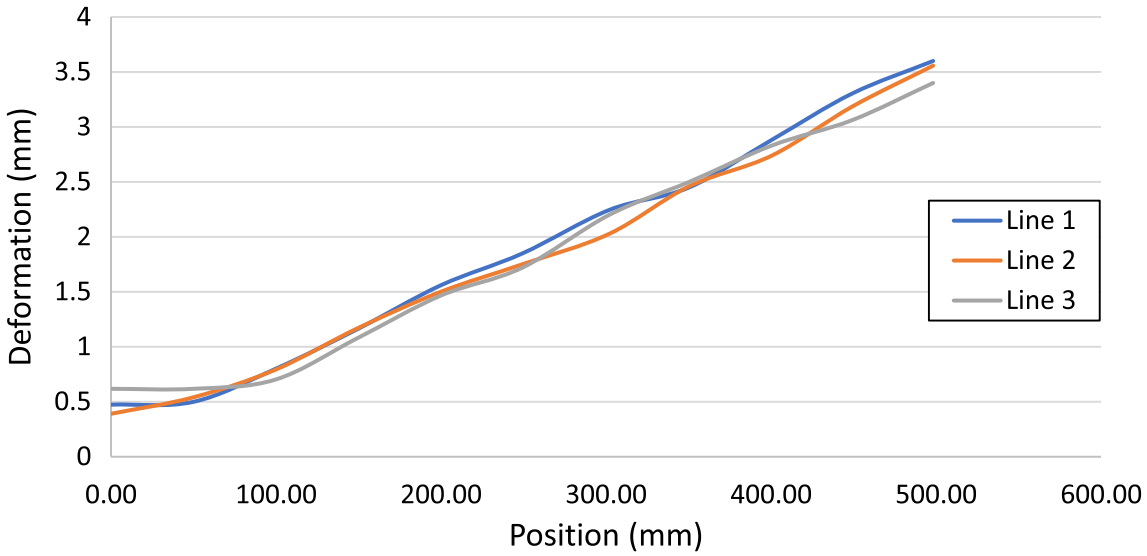

Fig. 15 Virtual deformation trend along the z-axis

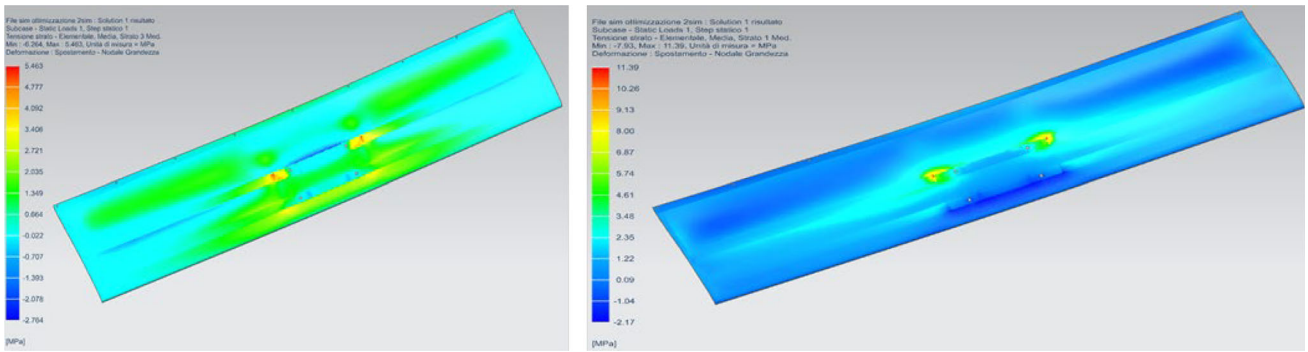

Fig. 16 Maximum stress (MPa) on the external (right) and internal (left) surfaces of the wing shell

Fig. 17 Maximum stress (MPa) on the Fillcore

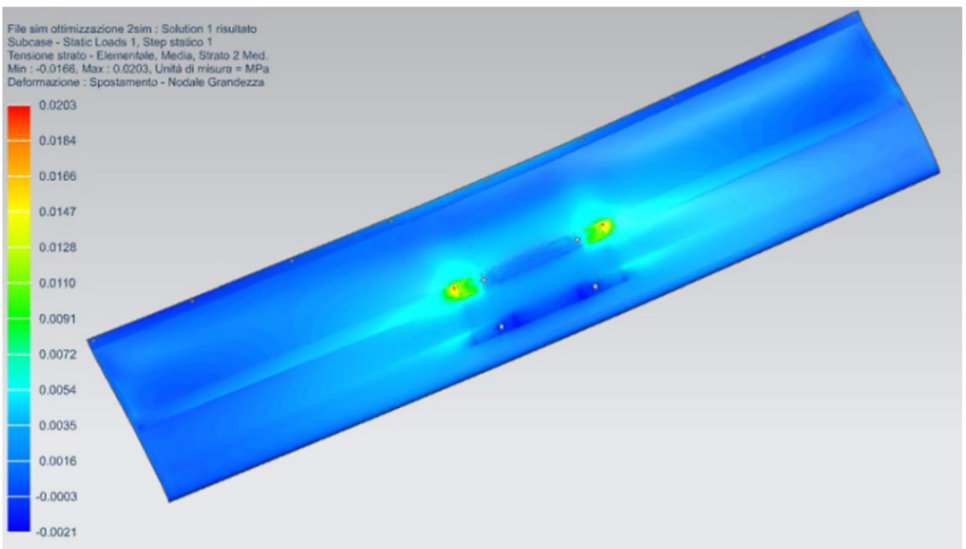

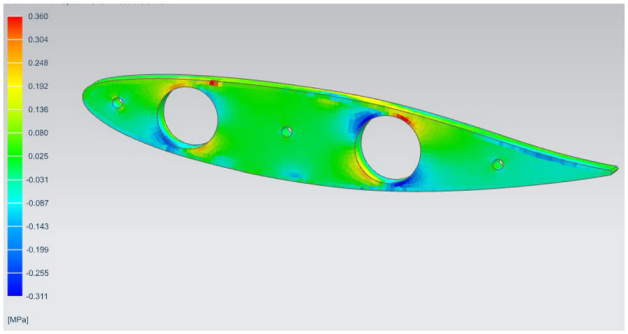

Fig. 18 Side cover's maximun stress (MPa)

indicated in Fig. 19), while in all the other parts, the tensions are not noteworthy (Fig. 20).

For the omega, only one layer is to be analyzed: in the central area, the tensional state presents a weak compression that decreases towards the ends, while where the inserts are placed, areas subjected to compression are present. In fact, the same tensions characterize the Ergal attachment areas that are discharged on the omega where they are connected (as illustrated in Fig. 22).

4 Product optimization

The aim of the proposed method is to optimize the product. Different optimizations can be achieved according to the objective of the analysis. Mass or displacement reduction, resistance increase, and failure index can be optimized in function of the analysis objective. The optimal design of the racing car wing is a highly complex process because it is necessary to consider many aspects that are incomparable, incalculable, and self-contradictory, which excludes their synchronized optimization [38].

For this case study, in accordance with competition regulations, the optimization involved minimizing the mass, setting the constraints of maximum displacement to 5 mm and failure index to 0.8 mm.

The optimization approach was divided into two stages. The lamination parameters and total laminate thickness were used as design variables in the first stage. The material properties were used in the second stage. In this case study, the fibers orientations used to build the actual layup for the laminate were constant.

Starting with the result validation (presented in the previous chapter), different laminate layers were simulated. For each configuration, the values of maximum displacement and failure index were recorded.

For material optimization, different analyses were done. For each material property, three different steps were considered: the starting value, the value of more than 10%, and the value of less than 10%.

Figures 21, 22 and 23 show the material properties considered in the analysis.

For the surface of the wing, the optimization affects both composite layers, while the Fillcore layer is left unchanged because it is made of homogeneous, isotropic material with little structural relevance. A continuous range of variation between 0.2 and 1.5 mm is set, and the choice of material among all those just created is made, including the original one.

It is possible to optimize the orientation angle of the layer. However, when working with a bidirectional fabric, this parameter has no influence on the results and is omitted. The objective of this optimization phase is the reduction of the total wing mass.

The constraints to be respected are the breaking index, which must not exceed the safety condition with a value of 0.8. Further, a minimum mass constraint is not set. For the

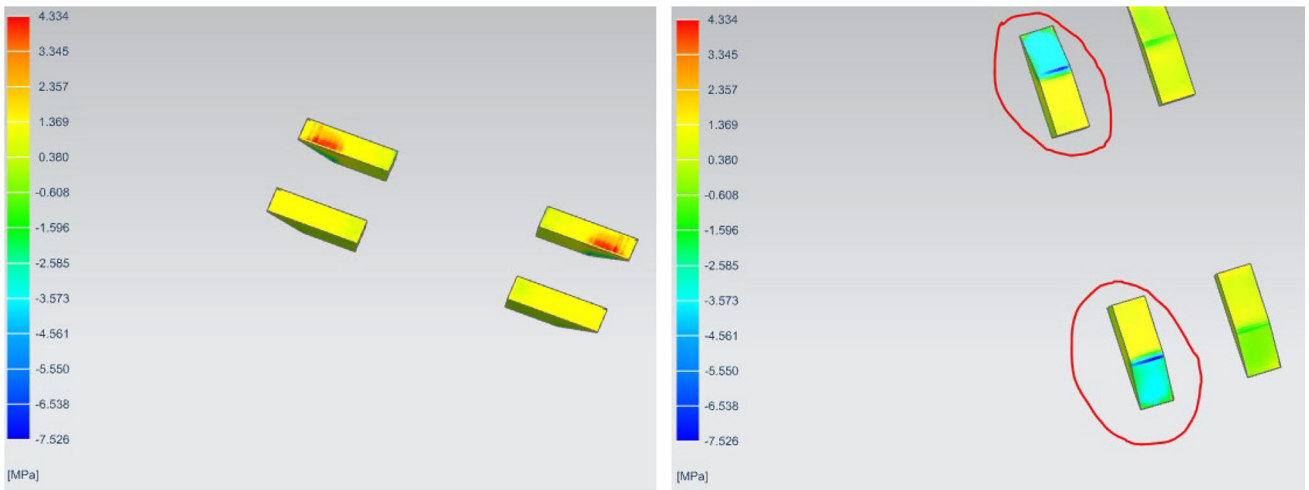

Fig. 19 Ergal insert stress (MPa)

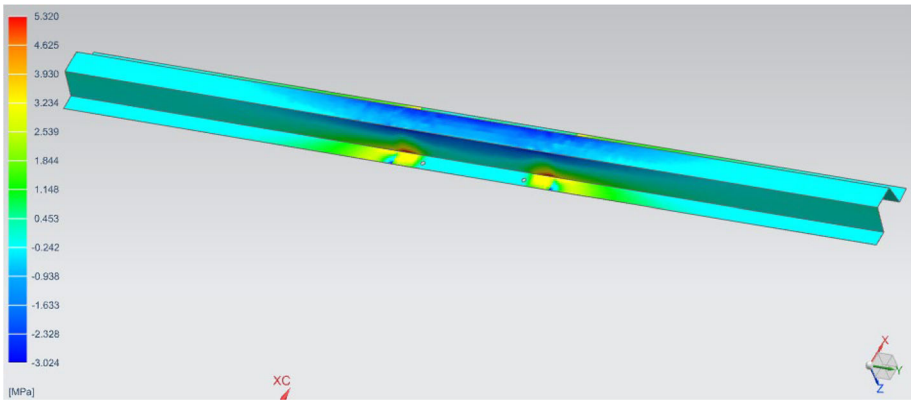

Fig. 20 Omega stress (MPa)

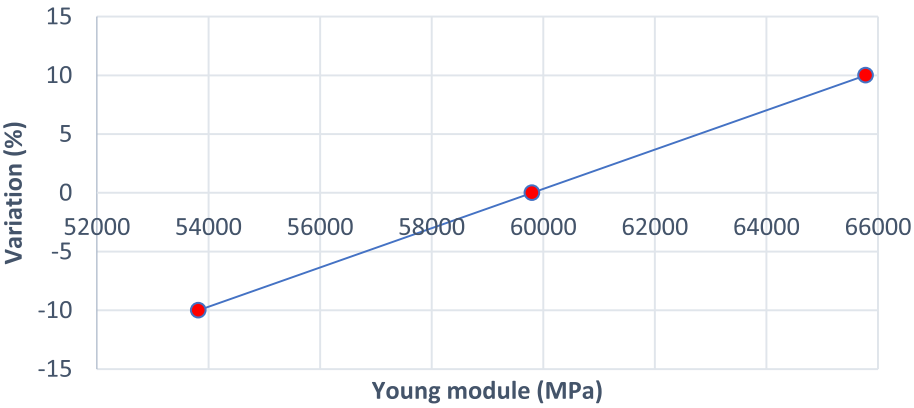

Fig. 21 Trend of Young's modulus in x-direction, E1

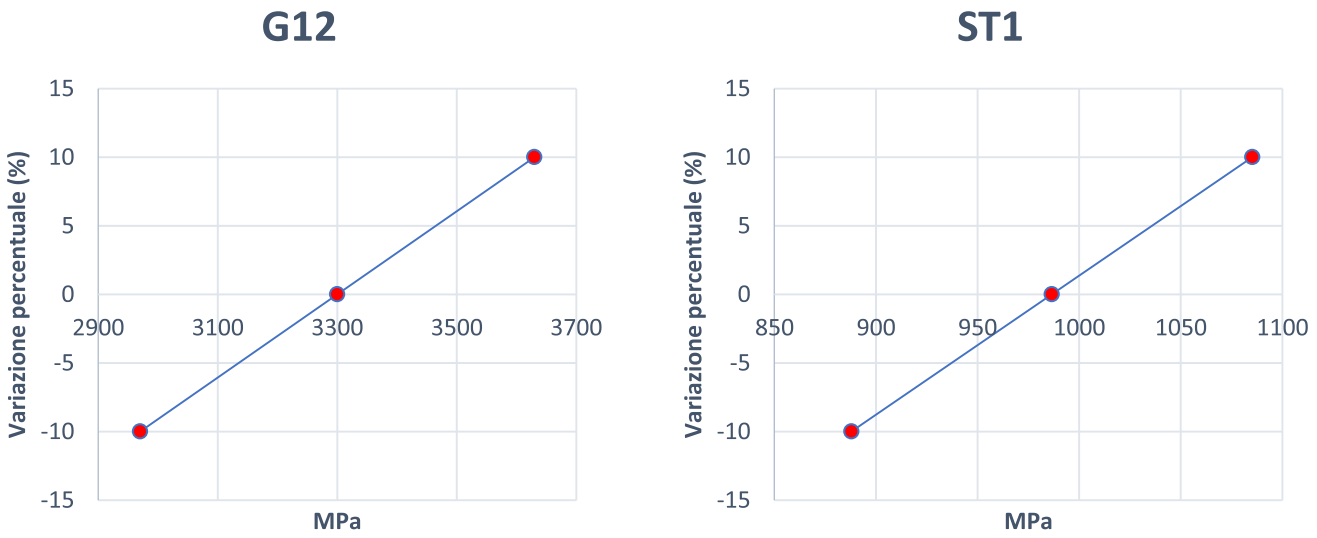

Fig. 22 Trend of the shear modulus of G12 and ST1

assignment of the load to the structure, it is not possible to accurately evaluate the part of the total load on the individual components. In the optimization section, a linear load must be set that is not easily attributable to the pressure used previously.

After various tests, a load of 20 N/mm was chosen. The iterative optimization process generates five configurations, ranging from the best to the worst, with relative characteristics. These candidates are presented in the tables with their respective data (Tables 6 and 7).

The optimization results show solutions that are similar to each other. In any case, the best configuration is identified. For the lower wing surface, the best configuration is solution 3, even if it has a higher mass than solutions 1 and 2. It

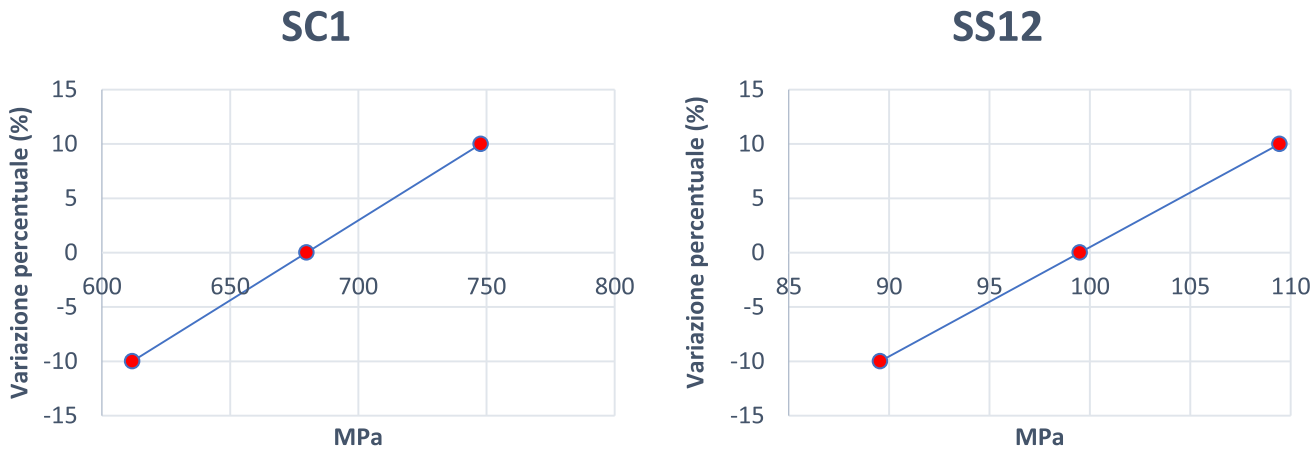

Fig. 23 Trend of Young's modulus in x-direction, E1

Table 6 Optimization result of the lower surface (load: 20 N/mm XY planes)

Configuration	Material	Thickness (mm)	Mass (kg)	Error index
Solution 1				
Layer 3	GG380T (+ 10% SC1)	0.2	3.43E − 01	0.765
Layer 1	GG380T (+ 10%)	0.309		
Solution 2				
Layer 3	GG380T (+ 10% SC1)	0.2	3.55E − 01	0.701
Layer 1	GG380T (+ 10%)	0.309		
Solution 3				
Layer 3	GG380T (+ 10%)	0.309	3.56E − 01	0.683
Layer 1	GG380T (+ 10% SS12)	0.2		
Solution 4				
Layer 3	GG380T (+ 10% SS12)	0.2	3.57E − 01	0.688
Layer 1	GG380T (+ 10% SS12)	0.331		
Solution 5				
Layer 3	GG380T (+ 10% ST2)	0.2	3.59E − 01	0.689
Layer 1	GG380T (+ 10% SS12)	0.333		
Start configuration				
Layer 3	GG380T	0.4	5.39E − 01	0.549
Layer 1	GG380T	0.4		

shows a lower error index, guaranteeing greater safety. The same consideration can be made for the upper surface, the best configuration is solution 2.

As described above, the omega is made of a single layer, and as evidenced by the data in Table 8, the best configuration is solution 2.

With optimization, the breaking coefficient for all three components is 0.75, and there is an overall weight reduction of 0.442 kg, which is 32% of the initial weight of the carbon layers. The table below provides a summary of the choice of candidates.

The optimized models were also simulated with the same loads and constraints presented previously. In particular, Fig. 24 shows the trend of the tensions of the nonoptimized model, the optimized model, and the shells and omegas that compose the wing study (Table 9).

In Fig. 24, the different components maintain the same state of loading (tension or compression). However, the optimized model produces different modulus values. It is possible to note an increasing value because, for the different components, the optimized model is made with a lower thickness. However, the maximum value is 50 MPa for the maximum principal stress, which is significantly under yield strength or tensile strength.

In addition to the stress trend, it is necessary to evaluate the maximum displacement.

Table 7 Optimization result of the upper surface (load: 20 N/mm XY planes)

Configuration	Material	Thickness (mm)	Mass (kg)	Error index
Solution 1				
Layer 3	GG380T (+ 10%)	0.309	3.42E − 01	0.761
Layer 1	GG380T (+ 10% E2)	0.2		
Solution 2				
Layer 3	GG380T (+ 10% SS12)	0.311	3.44E − 01	0.744
Layer 1	GG380T (+ 10%)	0.2		
Solution 3				
Layer 3	GG380T (+ 10% SS12)	0.311	3.45E − 01	0.752
Layer 1	GG380T (+ 10% E2)	0.2		
Solution 4				
Layer 3	GG380T (+ 10% SS12)	0.311	3.44E − 01	0.751
Layer 1	GG380T (+ 10% SC2)	0.2		
Solution 5				
Layer 3	GG380T (+ 10% SS12)	0.2	3.59E − 01	0.750
Layer 1	GG380T (+ 10% SS12)	0.333		
Start configuration				
Layer 3	GG380T	0.4	5.38E − 01	0.549
Layer 1	GG380T	0.4		

Table 8 Optimization result of the omega (load: 20 N/mm XY plane)

Configuration	Material	Thickness (mm)	Mass (kg)	Error index
Solution 1				
Layer 1	GG380T (+ 10%)	0.623	2.37E − 01	0.778
Solution 2				
Layer 1	GG380T (+ 10% SS12)	0.623	2.37E − 01	0.773
Solution 3				
Layer 1	GG380T (+ 10% G12)	0.678	2.58E − 01	0.793
Solution 4				
Layer 1	GG380T (+ 10% E2)	0.678	2.57E − 01	0.792
Solution 5				
Layer 1	GG380T (+ 10% ST2)	0.678	2.58E − 01	0.791
Start configuration				
Layer 1	GG380T	0.8	3.05E − 01	0.568

Figure 22 shows the trend of wing displacement in the external point (zones of maximum displacement) in function of the wing shell layer's thickness. The thicknesses of the omega (0.8 mm) and the material were kept constant, while the thicknesses of the layers of the shell varied from 0.1 to 0.6 mm.

A nonlinear relationship is highlighted between displacement and thickness. In fact, towards the lower values, the slope of the curve obtained is greater than that of the trend line. This means that the reduction in wing surface thickness has a greater influence than linear-type dependence. With greater thicknesses, the behaviour is opposite, with the slope of the straight line being higher than that of the curve. Only in the central part are the curve and straight line observed to be almost parallel to a linear trend. It can also be observed that while moving towards a thickness of 0.1 mm, the displacement begins to become important. Moreover, if the load or a few external conditions were to increase slightly, the displacement of 5 mm could be exceeded, which, in this analysis, is the maximum acceptable value (Fig. 25).

The same trend is found for the thickness of the omega, maintaining the layers of the shells at constant (0.4 mm) and varying the omega between the following thicknesses: 0.3, 0.5, 0.8, and 1 mm. Again, the materials are kept unchanged,

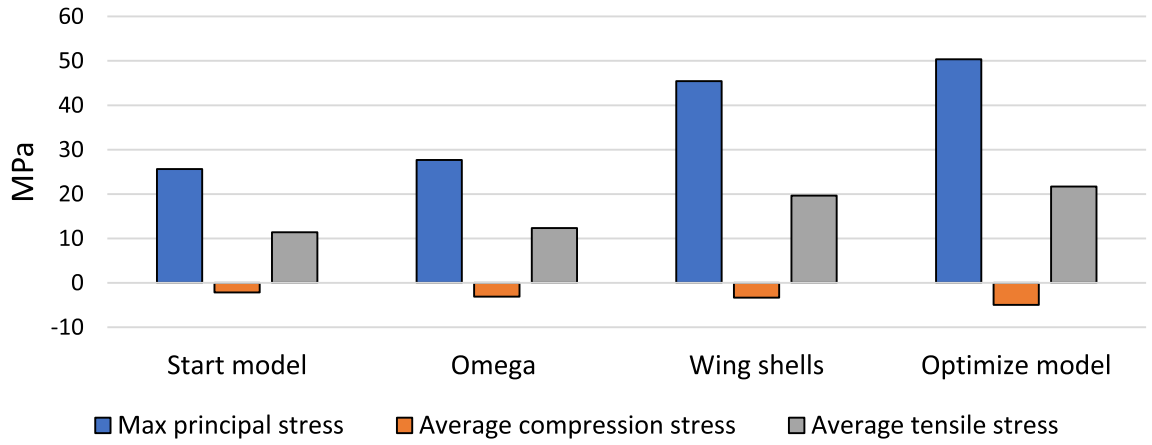

Fig. 24 Stress trend in the most stressed layer

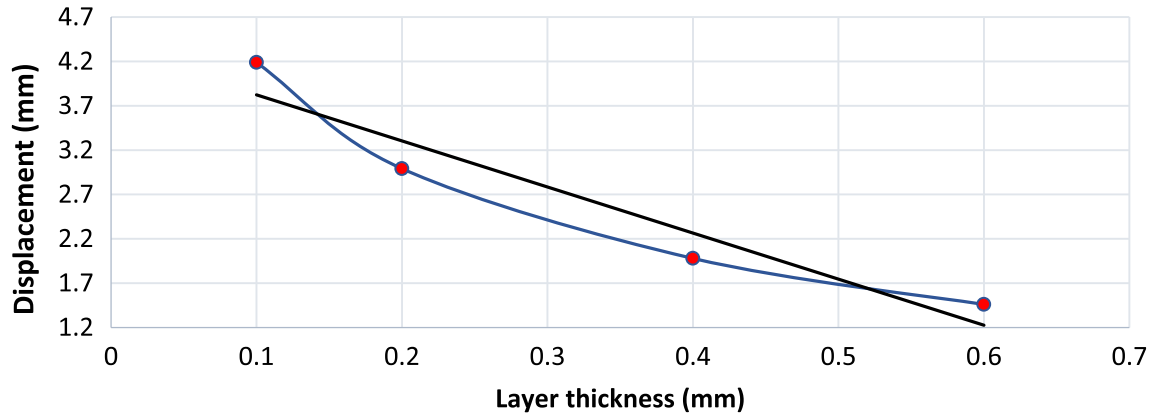

Fig. 25 Relationship between the thickness and displacement of the shell component

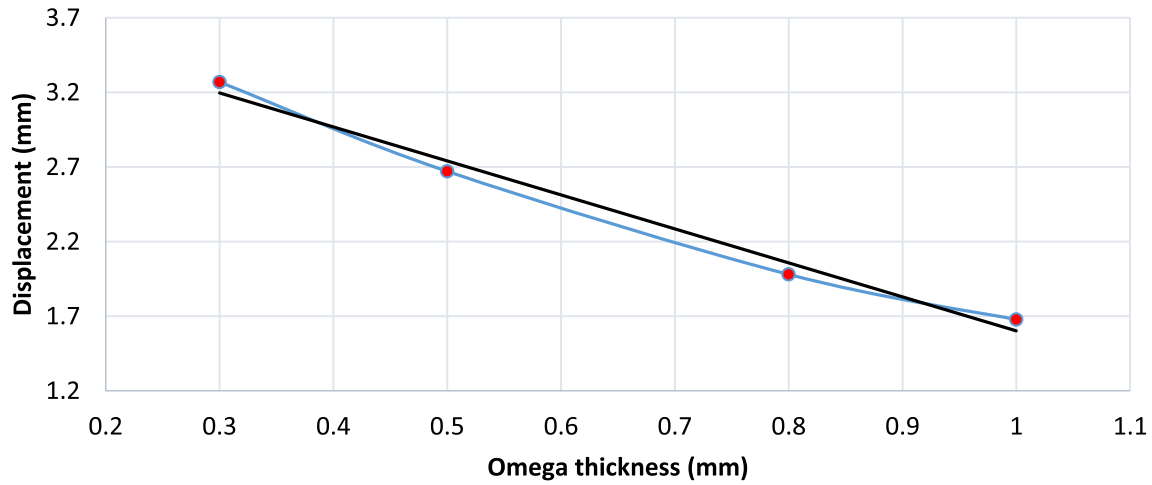

Fig. 26 Relationship between the thickness and displacement of the omega component

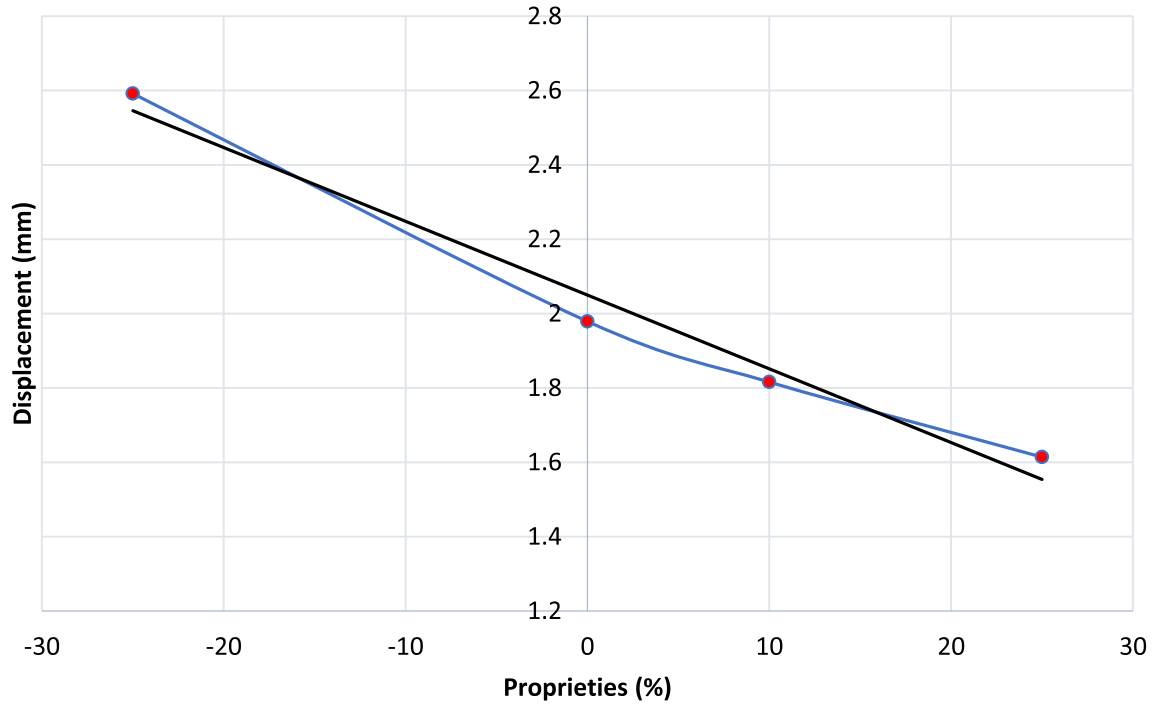

Fig. 27 Relationship between material properties and displacement

Table 9 Optimization result

Component	Starting model	Optimized model	Difference
Wing lower surface			
Failure index	0.549	0.683	+ 0.134
Weight (kg)	0.539	0.356	− 0.183
Wing upper surface			
Failure index	0.549	0.744	+ 0.195
Weight (kg)	0.538	0.344	− 0.194
Omega			
Failure index	0.568	0.773	+ 0.205
Weight (kg)	0.305	0.237	− 0.068

as shown in Fig. 26. The figure highlights a similar trend in the thickness of the layer. In this case, the linear trend line is closer to the experimental curve than that of the thickness of the shells. This affirms that the function linking the displacement of the wing and the thickness of the omega of reinforcement is almost linear.

As the last test, the variation of the displacement is analyzed as a function of the properties' material variation, which constitute both the layers of the wing shells and the omega without modifying the thicknesses of all the interesting parts. Four tests were performed: the first decreased all the parameters of GG380T by 25%; the second left them unchanged; and the third and fourth increased these values by 10 and 25%, respectively. Figure 27 shows a linear trend between displacement and material properties. The curve in Fig. 27 is flatter than that in the previous figures, which relates displacements to thicknesses. This means that for this application, the important thing is to consider the thicknesses that have a significant influence on the displacements. On the one hand, the properties of the materials have a greater influence on the tensions and the rupture index, which, as seen in the results analysis, do not assume unfavourable values for structural strength.

5 Conclusion

This paper presents an innovative approach based on the interaction of different aspects related to the world of manufacturing carbon fibre products. Material characteristics, the definition of the number of layers, drape analysis, and FEM simulations support designers in optimal product definition.

The analysis of a real case study involving a wing of a Formula 4 vehicle allowed this study to validate the proposed approach. The starting point was a real wing that is currently used in an actual race. Through experimental tests, it was possible to understand the real behaviour of the wing subjected to specific static loads. The same conditions were reproduced using a FEM tool to validate the numerical model.

The objective of the study is to show that, using a complex methodology that considers all the factors present during

the design cycle, it is possible to optimize the current products on the market. In particular, the objective of the study is wing mass reduction without compromising mechanical performance and Formula 4 regulation limits. The results show that it is possible to reduce the mass by approximately 10% by optimizing the design process.

One of the main limitations of this study is the extension of the validity of the numerical model for all carbon fibre products. The high number of variables present in composite materials makes the experimental validation of simulations necessary, slowing and complicating the product development process.

Other limitations can result from manufacturing processes. In general, there is no standard production process for composite materials. However, in function of different production volumes, durations to market, budgets and costs, and customer needs, different methods can be used to obtain various mechanical properties for the final product. Therefore, it is necessary to develop advanced optimization tools (e.g., based on artificial intelligence techniques) capable of also considering these aspects.

Future researchers can undertake not only the optimization of mass or deformation but also an analysis of environmental and economic aspects. The introduction of new materials and the implementation of these in real case studies can lead to significant improvements in the artefacts made of composite material.

Author contributions The author confirms sole responsibility for the following: study conception and design, data collection, analysis and interpretation of results, and manuscript preparation.

Funding Open access funding provided by Università degli studi di Bergamo within the CRUI-CARE Agreement.

Declarations

Conflict of interest The authors declare that they have no known competing financial interests or personal relationships that have influenced the work reported in this paper.

References

1. Cartwright, J.: Big stars have weather too. IOP Publishing PhysicsWeb. http://physicsweb.org/articles/news/11/6/16/1 (2007). Accessed 26 June 2007
2. Hu, J., Zhang, K., Yang, Q., et al.: An experimental study on mechanical response of single-lap bolted CFRP composite interference-fit joints. Compos. Struct. **196**, 76–88 (2018)
3. Nabipour, H., Wang, X., Hu, Y.: Carbon fiber-reinforced composites based on an epoxy resin containing Schiff base with intrinsic anti-flammability, good mechanical strength and recyclability. Eur. Polym. J. (2023). https://doi.org/10.1016/j.eurpolymj.2023.112166
4. Shamsuri, A.A., Yusoff, M.Z.M., Abdan, K., Jamil, S.N.A.M.: Flammability properties of polymers and polymer composites combined with ionic liquids. e-Polymers (2023). https://doi.org/10.1515/epoly-2023-0060
5. Shen, J., Liang, J., Lin, X., Lin, H., Yu, J., Wang, S.: The flame-retardant mechanisms and preparation of polymer composites and their potential application in construction engineering. Polymer (2021). https://doi.org/10.3390/polym14010082
6. Tsai, S.W., Wu, E.M.: A general theory of strength for anisotropic materials. J. Compos. Mater. **5**, 58–80 (1971)
7. Bahei-El-Din, Y.A.: Multiscale transformation field analysis of progressive damage in fibrous laminates. Int. Mult. Comput. Eng. (2010). https://doi.org/10.1615/IntJMultCompEng.v8.i1.60
8. Jones, Robert M.: Mechanics of composite materials, engineering & technology physical sciences. CRC Press, Boca Raton (2018). https://doi.org/10.1201/9781498711067
9. Tang, Z.X., Postle, R.: Mechanics of three-dimensional braided structures for composite materials—Part I: fabric structure and fibre volume fraction. Compos. Struct. **49**, 451–459 (2000)
10. Huang, Z.M., Ramakrishna, S.: Towards automatic designing of 2D biaxial woven and braided fabric reinforced composites. J. Compos. Mater. **36**, 1541–1579 (2002)
11. Donadon, M.V., Falzon, B.G., Iannucci, L., Hodgkinson, J.M.: A 3-D micromechanical model for predicting the elastic behaviour of woven laminates. Compos. Sci. Technol. **67**, 2467–2477 (2007)
12. Chun, H.J., Son, J., Kang, K.T., Byun, J.H., Um, M.K., Lee, S.K.: Prediction of elastic properties for woven z-pinned composites. Compos. B **64**, 59–71 (2014)
13. Kamiński, M., Pawlak, A.: Sensitivity and uncertainty in homogenization of the CFRP composites via the response function method. Compos. Struct. **118**, 342–350 (2014)
14. Kamarudin, K.A., Ismail, A.E.: Prediction of elastic properties for unidirectional carbon composites: periodic boundary condition approach. Appl. Mech. Mater. **773–774**, 262–266 (2014)
15. Yang, X., Gao, X., Ma, Y.: Numerical simulation of tensile behavior of 3D orthogonal woven composites (2018). Fibers Polym. **19**(3), 641–647 (2018). https://doi.org/10.1007/s12221-018-7975-8
16. Sun, Q., Meng, Z., Zhou, G., Lin, S.P., Kang, H., Keten, S., et al.: Multi-scale computational analysis of unidirectional carbon fiber reinforced polymer composites under various loading conditions. Compos. Struct. **196**, 30–43 (2018)
17. Todoroki, A., Ishikawa, T.: Design of experiments for stacking sequence optimizations with genetic algorithm using response surface approximation. Compos. Struct. (2004). https://doi.org/10.1016/j.compstruct.2003.09.004
18. Hajmohammad, M.H., Salari, M., Hashemi, S.A., Esfe, M.H.: Optimization of stacking sequence of composite laminates for optimizing buckling load by neural network and genetic algorithm. Indian J. Sci. Technol. (2013). https://doi.org/10.17485/IJST/2013/V6I8/36346
19. Butler, R., Williams, F.W.: Optimum design using VICONOPT, a buckling and strength constraint program for prismatic assemblies

of anisotropic plates. Comput. Struct. (1992). https://doi.org/10.1016/0045-7949(92)90511-W
20. Liu, X., Featherston, C.A., Kennedy, D.: Two-level layup optimization of composite laminate using lamination parameters. Compos. Struct. (2019). https://doi.org/10.1016/j.compstruct.2018.12.054
21. Le Riche, R., Haftka, R.T.: Optimization of laminated stacking sequence for buckling load maximization by genetic algorithm. AIAA J. (1992). https://doi.org/10.2514/3.11710
22. Russo, D., Spreafico, C.: Investigating the multilevel logic in design solutions: a function behaviour structure (FBS) analysis. Int. J. Interact. Des. Manuf. (2023). https://doi.org/10.1007/s12008-023-01251-6
23. Almeida, F.S., Awruch, A.M.: Design optimization of composite laminated structures using genetic algorithms and finite element analysis. Compos. Struct. (2009). https://doi.org/10.1016/j.compstruct.2008.05.004
24. Chen, S., Lin, Z., An, H., Huang, H., Kong, C.: Stacking sequence optimization with genetic algorithm using a two-level approximation. Struct. Multidiscip. Optim. (2013). https://doi.org/10.1007/s00158-013-0927-4
25. Cherouat, A., Borouchaki, H., Billoët, J.-L.: Geometrical and mechanical draping of composite fabric. Rev. Euro. des Elém. Finis **14**, 693–707 (2005)
26. Brydson, J.: Plastics materials. Butterworth-Heinemann, Oxford, UK (1999)
27. Žmindák, M., Dudinský, M.: Computational modelling of composite materials reinforced by glass fibers. Procedia. Eng. **48**, 701–710 (2012)
28. Rothon, R.N.: Particulate Fillers for Polymers. Rapra Technology, Shawbury (2002)
29. Kant, T., Kant, T.: Composite mechanics in the last 50 years. http://www.ircc.iitb.ac.in/IRCCWebpage/rnd/PDF/TarunKant2010.pdf
30. Mack, C., Taylor, H.: The fitting of woven cloth to surfaces. J. Text. Inst. **8**, 477–488 (1956)
31. Pickett, A.K., Creech, G., de Luca, P.: Simplified and advanced simulation methods for prediction of fabric draping. Rev. Eur. Des. Elém. (2005). https://doi.org/10.3166/reef.14.677-69
32. Cherouat, A., Borouchaki, H., Billoët, J.-L.: Geometrical and mechanical draping of composite fabric. Rev Euro des Elém Finis **14**, 693–707 (2005)
33. Broy, M., Denert, E. (eds.): Software Pioneers, Contribution of virtual simulation to industrialisation of carbon fibre-reinforced polymer (CFRP) composites for manufacturing processes and mechanical performance, pp. 10–13. Springer, Heidelberg (2002)
34. Daniel, C., Durand, C.: Composites Technologies for Transport 886 Applications: A Roadmap. Publisher, Place of Publication (2016). 7th framework Programme for NMP Theme"Advanced material textiles for reinforced structures for complex lightweight applications"August 2013-July 2016Project coordinator: Prof. Daniel CoutellierEditor: ENSIAMEISBN: 978-2-9559182-0-3 (5) (PDF) Composites technologies for transport applications: A roadmap. Available from: https://www.researchgate.net/publication/317936973_Composites_technologies_for_transport_applications_A_roadmap. Accessed 20 Jun 2024.
35. Liu, X., Gasco, F., Yu, W., Goodsell, J., Rouf, K.: Multiscale analysis of woven composite structures in MSC. Nastran. Adv Eng Softw **135**, 102677 (2019). https://doi.org/10.1016/j.advengsoft.2019.04.008
36. Akritas, M.G., LaValley, M.P.: 20 Statistical analysis with incomplete data: A selective review. In: Handbook of Statistics, 551–632. (1997)
37. Chen, X., Sun, X., Chen, P., Wang, B., Gu, J., Wang, W., Chai, Y., Zhao, Y.: Rationalized improvement of Tsai–Wu failure criterion considering different failure modes of composite materials. Compos. Struct. (2021). https://doi.org/10.1016/j.compstruct.2020.113120
38. Jureczko, M., Mrówka, M.: Multiobjective optimization of composite wind turbine blade. Mater. (2022). https://doi.org/10.3390/ma15134649